Charged Block Copolymer Mesogels

E. B. Zhulina†

Department of Physical and Colloid Chemistry, Wageningen Agricultural University, Dreijenplein 6, 6703 HB Wageningen, The Netherlands

Received April 1, 1993; Revised Manuscript Received July 6, 1993•

ABSTRACT: Equilibrium properties of mesogels—supermolecular networks, formed by symmetrical triblock copolymers with ionizable central blocks—are considered by scaling and self-consistent-field (SCF) arguments. We use the analogy between swelling elements of mesogels and polymer brushes to predict the swelling in selective solvents and deformational behavior of mesogels. It is shown that equilibrium interdomain distances in charged mesogels of various morphologies obey universal scaling laws. Reducing the solvent strength leads to an abrupt collapse of mesogels (phase transition of the first order) far below the Θ point. A detailed analysis of the intrinsic structure of lamellar mesogel is carried out within a SCF theory. As in neutral mesogels, swelling layers are inhomogeneous and their structure is sensitive to the fraction of bridging chains.

I. Introduction

A characteristic feature of di- and triblock copolymers, with long incompatible blocks, is their ability to form mesophases. The morphology of a microsegregated system is determined by the composition of the block copolymer molecules, the amount and selectivity of solvent, etc.[1,2] Block copolymer superstructures formed by triblock copolymers ABA manifest certain properties of physical gels due to the existence of bridging chains B connecting neighboring domains of the A component. These bridging chains provide the formation of a physical network of high functionality where the role of conventional cross-links is taken over by the A domains of the superstructure. Contrary to chemically cross-linked networks, the swelling of block copolymer mesophases leads to local rearrangement of superstructures accompanied by an increase in the average distance between neighboring chains. The fraction of bridging chains can also be varied. The swelling of mesophases in selective solvents can further lead to global change of the morphology of the superstructure (phase transitions of the *I* order).[3] Additional cross-linking of the insoluble component can be used to avoid the possible variation of the superstructure parameters in the process of swelling. Such cross-linking leads to the fixation of the fraction of bridging chains and the interchain distance. Mesogels will now be stable against the dissociation into separate aggregates in the swelling process and exhibit the properties of supermolecular networks. (The insoluble A domains are equivalent to the cross-links in conventional networks, where the number of bridging B chains per domain determines the "functionality" of each "cross-link".)

The theoretical analysis of neutral mesogels[4,5] utilized the analogy between conformations of blocks in mesophases with those of chains in polymer brushes. A scaling analysis provided the equilibrium swelling concentrations of spherical, cylindrical, and planar mesogels, whereas the self-consistent-field theory of brushes[6-8] applied to lamellar mesogel gave an opportunity to calculate the equilibrium fraction, q, of bridging chains and to consider the internal structure of swollen B layers. It was shown that swelling layers are inhomogeneous: their central zones contain only segments of bridging chains, and loops are excluded from these central zones. In this approach elastic and shear moduli of lamellar single-crystal mesogel were calculated.

The aim of this paper is to extend the theoretical analysis of mesogels for the case that the swelling blocks B of the triblock copolymer ABA carry ionizable groups, which can be charged in the process of swelling. Combination of long-range electrostatic repulsion between charged monomers with conventional short-range volume interactions between noncharged units leads to new regimes of behavior in polymer brushes and mesogels. In particular, collapse of polyelectrolyte polymer brushes caused by inferior solvent strength occurs as phase transition of the first order contrary to smooth collapse in neutral brushes.[10,11] Jumpwise change in brush thickness takes place far below the Θ point when attractive pair interactions become strong enough to overcome electrostatic repulsion between charges. Abrupt collapse is, thus, expected for charged mesogels as well. Experimentally, collapse of mesogels can be observed by small-angle scattering techniques developed for conventional block copolymer systems. Moreover, mesogels can, probably, provide wider opportunities for experiment than individual polymer brushes. Due to possible macroscopic size of mesogel samples, their deformation behavior can be tested as well. The charged groups are expected to effect the properties of mesogels both at weak and strong deformations.

This paper is organized as follows. In section II the model of charged mesogels is described. The scaling-type analysis of mesogels of various morphologies is carried out in section III, and the blob picture is introduced. A more detailed self-consistent-field theory of lamellar mesogel is developed in section IV. The paper is concluded in section V by collecting the most important results.

II. Model

Consider a melt of symmetrical triblock copolymers ABA under the conditions of microphase segregation. Let $N_A \gg 1$ and $N_B \gg 1$ be the numbers of units of the A and B blocks, respectively. (Chain segment of length a equal to chain thickness is chosen as a unit.) Both blocks are assumed to have units of equal sizes, $a_A = a_B = a$, and be of the same flexibility ($A/a = 1$ where A is the Kuhn segment). The central B block is assumed to contain ionizable groups which are not charged under the conditions of a melt state. Thus, microphase segregation is not effected by the presence of ionizable groups and occurs as in neutral block copolymers, i.e., with the formation of well-defined mesophases with narrow interfacial regions.

† Permanent address: Institute of Macromolecular Compounds, Russian Academy of Sciences, St. Petersburg 199004, Russia.

• Abstract published in *Advance ACS Abstracts*, October 15, 1993.

0024-9297/93/2226-6273$04.00/0

The equilibrium morphology of a mesophase is determined by the block copolymer composition, $k = N_B/2N_A$. Three conventional types of mesophases (and corresponding mesogels) are considered: lamellar ($i = 1$), cylindrical ($i = 2$), and spherical ($i = 3$). Lamellar structure consisting of planar domains of A and B components is known to be the most stable one at $k = 1$. At $k \gg 1$ spherical or cylindrical domains of minor component A are formed in the matrix of major component B. In the narrow interface approximation, the domain radius, R, and the average area of interface per chain, σ, scale as[6]

$$R/a \approx N_A^{2/3}\omega_i(k)^{-1/3} \sim N_A^{2/3} \quad (1)$$

$$\sigma/a^2 \approx N_A^{1/3}\omega_i(k)^{1/3} \sim N_A^{1/3} \quad (2)$$

where $\omega_i(k)$ is a nonpower function of k. The interdomain spacing is given by

$$H/a \approx k^{1/i}R/a \sim N_A^{2/3} \quad (3)$$

Thus, in well-defined superstructures of block copolymers, both blocks A and B are stretched normally to the interfaces and form polymer brushes of corresponding morphologies.

Let q be the average fraction of bridging B blocks per A domain. The equilibrium value of q, q_{eq}, was calculated[5] for the particular case of lamellar geometry. In this paper, however, q will be treated as an independent parameter since slow kinetics of microphase segregation can provide $q \neq q_{eq}$. The same refers to the value of σ which can differ from σ_{eq} given by eq 2. Thus, the initial mesophase formed at a given dry melt stage is characterized by the following parameters: morphology i ($i = 1$–3), interfacial area per chain σ, the fraction q of bridging chains.

As was discussed in refs 4 and 5, mesogel formation demands an additional fixation of the structural parameters of the initial mesophase (σ and q). For example, selective chemical cross-linking of block A can be used. The swelling of mesogel occurs in this case at constant values of σ and q as in the supermolecular network formed by cross-linked A domains and bridging B chains. We assume that in the process of swelling of mesogels by highly selective dielectric solvent (ϵ_s being its dielectric constant), ionizable groups are charged. Let m be the number of uncharged B units between neighboring charged groups on a B chain. For a weakly charged polyelectrolyte B block direct electrostatic repulsion does not lead to electrostatic stiffening of the B chain provided[12]

$$\frac{e^2}{\epsilon_s kT a\sqrt{m}} = \frac{l_B}{a\sqrt{m}} \ll 1 \quad (4)$$

Here e is elementary charge and $l_B = e^2/\epsilon_s kT$ is the Bjerrum length. Assuming $l_B \approx a$, we omit it from further considerations.

Due to the total electroneutrality of the system, there are $Q = N_B/m$ mobile counterions per chain distributed in the dielectric medium. As is known,[13,14] the selective charging of block copolymer molecules improves the compatibility of the system and smooths the interfacial regions in the microsegregated state. Due to a preliminary cross-linking of the A block, the effects of broadening the boundaries between A and B components can be neglected in mesogels. Thus, mobile counterions can be considered as localized in the swollen B layers provided that the dielectric solvent is highly selective and does not penetrate into the insoluble A domains.

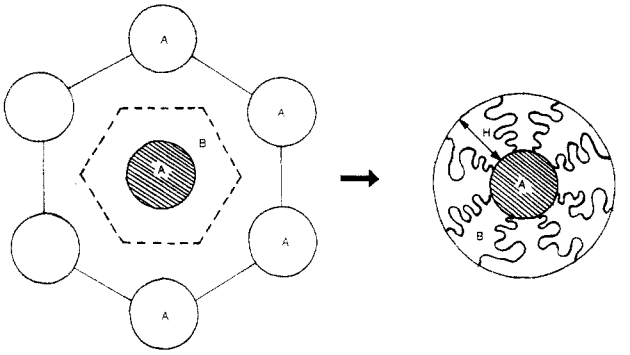

Figure 1. Schematic representation of a swelling element of a block copolymer mesogel and a polymer brush of corresponding geometry.

III. Scaling-Type Analysis of Mesogels

In this section only asymptotical power laws of mesogel characteristics are considered. Numerical coefficients and nonpower dependencies are ignored. For simplicity all B blocks are assumed to form bridges between neighboring domains ($q = 1$), and, thus, the q dependence of the mesogel parameters is omitted here.

Segment Density Profile and Equilibrium Swelling Concentration. In order to calculate the equilibrium swelling concentration, ϕ^*, of a mesogel, the analogy between a swelling element and a polymer brush of corresponding morphology is utilized (see Figure 1). Since all B blocks are assumed to form bridges, one can envision a swelling element of a mesogel as a polymer brush formed by chains of $N = N_B/2$ units grafted at one end onto the surface of an A domain and the other ends fixed at the outer boundary of the brush. Such a brush is immersed in a dielectric solvent and surrounded by an impermeable shell of thickness H providing localization of all mobile counterions inside the brush.

The equilibrium swelling concentration of such a system can be obtained by minimization of the free energy functional, ΔF, following the arguments of refs 10 and 11. For a charged brush the free energy

$$\Delta F = \Delta F_{el} + \Delta F_{ion} + \Delta F_{conc} \quad (5)$$

incorporates entropy losses due to chain stretching, ΔF_{el}, the translational entropy of counterions, ΔF_{ion}, and nonelectrostatic volume interactions, ΔF_{conc}. Mean-field expressions for all components of the free energy are used throughout this paper.

Let $\phi(r)$ be the volume fraction of polymer units at a distance r from the center of a given domain. Then the elastic free energy per chain is given by[6,11]

$$\Delta F_{el} = \frac{3}{2a^2}\int_R^{R+H}\left(\frac{dr}{dn}\right)dr = \frac{3}{2}\int_R^{R+H}\left[\frac{I_i a}{c_i\phi(r)\, r^{i-1}}\right]dr \quad (6)$$

where i determines the geometry of a mesogel, ($c_i r^{i-1}\, dr$) is the radial part of its elementary volume ($c_1 = 1$; $c_2 = 2\pi$; $c_3 = 4\pi$), and $I_i = c_i R^{i-1}/\sigma$ is the angular, linear, and surface grafting density for $i = 3$, 2, and 1, respectively. (Here and below the free energy is expressed in units of kT.)

The electrostatic contribution

$$\Delta F_{ion} = \frac{1}{a^3 I_i}\int_R^{R+H}\phi_{ion}(r)\ln[\phi_{ion}(r)]c_i r^{i-1}\, dr \quad (7)$$

is dominated by the translational entropy of the counterions distributed in a slit of width H with the profile $\phi_{ion}(r)$. Ignoring correlation effects in the counterion distribution[10] and using the condition of average local

Table I. Scaling Dependencies of H^* and Φ^* in Various Solvents

	good solvent	Θ solvent	precipitant	
			$v > m^{-1/2}$	$v < m^{-1/2}$
		Neutral Mesogel		
H^*/a	$(vI_ia^{3-i})^{1/(i+2)}N^{3/(i+2)}$	$(w^{1/2}I_ia^{3-i})^{1/(i+1)}N^{2/(i+1)}$	$(I_ia^{3-i}wN\lvert v\rvert^{-1})^{1/i}$	
Φ^*	$v^{-i/(i+2)}(I_ia^{3-i})^{2/(i+2)}N^{-2(i-1)/(i+2)}$	$w^{-i/2(i+1)}(I_ia^{3-i})^{1/(i+1)}N^{(1-i)/(1+i)}$	$\lvert v\rvert/w$	
		Charged Mesogel		
H^*/a		$Nm^{-1/2}$		$(I_ia^{3-i}wN\lvert v\rvert^{-1})^{1/i}$
Φ^*		$(I_ia^{3-i})m^{i/2}N^{1-i}$		$\lvert v\rvert/w$

electroneutrality, one has $\phi_{ion}(r) = \phi(r)/m$ where $\phi(r)/m$ is the profile of immobilized charges on the polymer chains.

The last contribution to the free energy, ΔF_{conc}, is determined by nonelectrostatic volume interactions between units. For relatively loose brushes where only pair and ternary interactions are important,

$$\Delta F_{conc} = \frac{1}{a^3 I_i}\int_R^{R+H}[v\phi^2(r) + w\phi^3(r)]c_i r^{i-1}\,dr^1 \qquad (8)$$

where va^3 and wa^6 are the second and third virial coefficients of unit interactions.

Minimization of ΔF with respect to $\phi(r)$ under the constraint of conservation of the total number of units

$$\int_R^{R+H}\phi(r)\,c_i r^{i-1}\,dr = I_i N a^3 \qquad (9)$$

leads to the following equation for the profile $\phi(r)$

$$\frac{3a^4 I_i^2}{2c_i^2\phi^2(r)\,r^{2(i-1)}} = \lambda + \frac{1}{m}\ln\left[\frac{\phi(r)}{m}\right] + 2v\phi(r) + 3w\phi^2(r) \qquad (10)$$

where $\lambda = \lambda(H)$ is an indefinite Lagrangian multiplier. The translational entropy of mobile counterions dominates over nonelectrostatic interactions[9,10] under the conditions of a good or a Θ solvent at small m values (strongly charged brushes). Thus, the two last terms on the right-hand side of eq 10 can be omitted, and a power law dependence for $\phi(r)$ is obtained:

$$\phi(r) = \frac{I_i a^2 \Lambda}{c_i r^{i-1}}$$

where the constant Λ can be obtained from normalization condition (9) and is given by $\Lambda = Na/H$. Substituting $\phi(r)$ into eqs 6 and 7 and then minimizing the total free energy ΔF with respect to H, one obtains for the equilibrium thickness of the brush, $H_e \gg R$,

$$H_e \approx aN/\sqrt{m} \qquad (11)$$

and the equilibrium profile of polymer units

$$\phi_e^* = \frac{a^2 I_i\sqrt{m}}{r^{i-1}} \qquad (12)$$

Correspondingly, the equilibrium swelling concentration of a charged mesogel is given by

$$\phi_e^* \cong \frac{I_i N a^3}{H_e^{\,i}} \cong I_i a^3 m^{i/2} N^{1-i} \cong \left(\frac{a^2\sqrt{m}}{\sigma}\right)^i k^{1-i} \qquad (13)$$

It follows from eq 13) that for nonplanar layers ($i > 1$) ϕ_e^* decreases rapidly with increasing molecular weight, N. This leads to a corresponding increase in the Debye–Hückel radius

$$r_D \cong a(m/\phi_e^*)^{1/2}$$

However, even for a spherical geometry ($i = 3$) where r_D increases with N most rapidly, the necessary condition $r_D \ll H_e$ is fulfilled in a wide range of m values, $m \ll I_3^2$, where $I_3 \approx R^2/\sigma \gg 1$ is the total number of molecules in the A domain.

Reducing the charge density $1/m$ in polyelectrolyte block B leads to a less polyelectrolyte swelling (eqs 11 and 13). At weak charging when nonelectrostatic interactions between units dominate, the mesogel passes into the "quasineutral" regime. The equilibrium thickness of swelling layers and the distribution of units coincide in this case with those for neutral brushes. In particular, under the conditions of a good solvent ($v > 0$) the pair-interaction term dominates on the right-hand side of eq 10 to give[11]

$$\phi(r) \approx v^{-1/3}(I_i a^{3-i})^{2/3}(a/r)^{2(i-1)/3} \qquad (14)$$

In a Θ solvent ($v = 0$), where ternary contacts dominate,

$$\phi(r) \approx w^{-1/4}(I_i a^{3-i})^{1/2}(a/r)^{(i-1)/2} \qquad (15)$$

and under the conditions of precipitant, $v < 0$, where attractive pair interactions are balanced by repulsive ternary contacts,

$$\phi(r) = \text{const}(r) \approx |v|/w \qquad (16)$$

(This last expression is valid at $\phi \ll 1$ when higher order interactions can be neglected.) The corresponding thicknesses of swelling layers and equilibrium swelling concentrations are summarized in Table I.

Blob Picture. Let us introduce now a blob picture of polyelectrolyte mesogels. (Neutral mesogels were discussed in detail in ref 5.) It follows from eqs 11 and 12 that for all morphologies ($i = 1$–3) the charged bridging blocks are uniformly stretched normally to the interfaces,

$$\frac{dr}{dn} \cong \frac{I_i a^3}{\phi_e(r) r^{i-1}} \cong a\sqrt{m} \cong \frac{H_e}{N}$$

Thus, one can envision the B block as a string of N_b equal stretching blobs of size $\xi_s \cong a\sqrt{m}$, $H_e \cong \xi_s N_b$. Within a stretching blob a polymer chain is unperturbed and Gaussian so that each blob contains $N/N_b = n_b \cong (\xi_s/a)^2 \cong m$ units. Thus, there is one immobilized charge per blob (Figure 2). Stretched B chains fluctuate in lateral directions so that their lateral dimensions scale as $R_\perp \cong \xi_s N_b^{1/2}$.

Contrary to the situation in neutral brushes, these chains of blobs are not densely packed. For comparison the blob picture of a cylindrical brush in a Θ solvent and in precipitant are shown in Figure 2. Under the conditions of a Θ solvent ($v = 0$) blobs are also Gaussian, but their size $\xi \sim r$ increases to the periphery of the layer.[15,16] Under the conditions of precipitant, $v < 0$, the blob size ξ_c is independent of r, $\xi_c \cong a|v|^{-1}$, but now the blobs are densely packed.[17,18]

Contrary to neutral systems, charged mesogels exhibit a universal power law dependence for the equilibrium

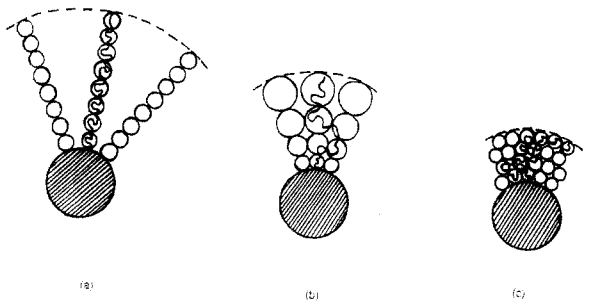

Figure 2. Blob picture of a swelling element of a charged cylindrical mesogel in the osmotic regime (a) and that of a neutral mesogel in a Θ solvent (b) and in precipitant (c).

thickness of the swelling layers, H_e, for all morphologies i. (The geometry effects only the numerical prefactor.) This is due to the fact that the osmotic force created by the mobile counterions that tends to increase H, $f_{ion} \approx kTN/mH$, scales in a similar way for all morphologies. Opposed by the elastic force of stretched chains, $f_{el} \approx kTH/Na^2$, it provides the dependence (11) and the corresponding blob picture of Figure 2.

A similar picture of a planar polyelectrolyte brush immersed in an infinite bulk of dielectric solvent was obtained earlier in refs 9 and 10. It was shown that in a wide range of conditions $\sigma/a^2 < N^2m^{-3/2}$ a charged brush conserves the major part of its mobile counterions inside the brush and, thus, its thickness is also given by eq 11. For rather loose brushes, however, a considerable part of mobile counterions leaves the brush and the brush thickness obeys another power law.[9]

For nonplanar brushes immersed in a bulk of solvent, counterions can also leave the brush (see, however, the discussion in ref 19) and the direct analogy between swollen charged mesogels and free charged brushes, thus, fails. (Note that localization of the mobile counterions in the swelling layers of mesogel is taken into account in our model by introducing an impermeable outer shell.)

Collapse of Charged Mesogels. The effect of solvent strength on the dimensions of a planar polyelectrolyte brush was analyzed in refs 10 and 19. Contrary to the smooth collapse of a neutral brush, the collapse of a charged brush was shown to occur abruptly as a first-order phase transition. This jumpwise diminishing of the brush thickness from its osmotic value, H_e, to that in its globular state, H_c, occurs far below the Θ point when the value of the second virial coefficient $|v| \cong 1/\sqrt{m}$. Thus, the same type of behavior is expected for a charged lamellar mesogel with inferior solvent strengths. Moreover, one should expect a jumpwise change in the dimensions of spherical and cylindrical mesogels as well, since H_e is independent of the morphology i (eq 11) and H_c diminishes with increasing i (see Table I).

In order to analyze the main features of these transitions, we ignore the concentration gradients in the swelling layers given by eqs 12 and 14–16 and simplify the model by using the average values of ϕ in all its components of the free energy ΔF. Within this approximation one has for the free energy per block B (provided that $H \gg R$ and that the chains are stretched)

$$\Delta F/N_B \cong \frac{a^4}{\sigma^2 k^{2-2/i}\phi^{2/i}} + \frac{1}{m}\ln\left(\frac{\phi}{m}\right) + v\phi + w\phi^2 \qquad (17)$$

where $k = N_B/2N_A$ and the numerical prefactor in the first term is omitted.

The equilibrium swelling concentration, ϕ^*, is determined then by the condition $\partial\Delta F/\partial\phi = 0$ to give

$$\frac{a^4k^{2/i-2}\phi^{2/i-1}}{\sigma^2} = v + 2w\phi + \frac{1}{m\phi} \qquad (18)$$

Equation 18 determines ϕ^* as a function of v, w, m, σ, and k. It is easy to check that retaining the corresponding terms in eq 18 one obtaines the same scaling dependencies for ϕ^* as those summarized in Table I. For simplicity we will assume below that $w = 1$ and omit it from further consideration.

In neutral layers ($m \to \infty$) eq 18 provides a smooth dependence of ϕ^* on v: $\phi^*(v)$ decreases monotonically with inferior solvent strength (see ref 11 for details). In charged brushes, however, the dependence $\phi^*(v)$ indicates an instability: it contains a looplike part in the range of negative values of v. The parameters of the corresponding critical point can easily be obtained from eq 18 with the conditions $\partial v/\partial\phi = \partial^2 v/\partial\phi^2 = 0$ to give

$$m_{cr} \cong k^{2(i-1)/(1+i)}(\sigma/a^2)^{2i/(i+1)}$$

$$|v_{cr}| \cong \phi_{cr} \cong (\sigma/a^2)^{-i/(i+1)}k^{-(i-1)/(i+1)} \qquad (19)$$

The spinodal equation, $\partial v/\partial\phi = 0$, gives the following asymptotics for the two branches at $m < m_{cr}$

$$\phi_1 \cong 1/\sqrt{m}; \qquad \phi_2 \cong (ma^4/\sigma^2)^{i/2}k^{1-i} \qquad (20)$$

As is seen from eq 19, the critical point parameters are rather sensitive to the geometry of the system. At fixed values of k and σ polyelectrolyte effects manifest first in spherical, then in cylindrical, and, finally, in lamellar morphologies: m_{cr} increases, while $|v_{cr}| \approx m_{cr}^{-1/2}$ decreases with i increasing.

Polyelectrolyte effects stabilize a brush against collapse at $m < m_{cr}$, and a jumpwise decrease in dimensions occurs only in the range of $|v| > v_{cr}$. In order to estimate the transition point $|v_0|$ where the abrupt change in the brush thickness takes place, the blob picture of Figure 2 is utilized.

As was already mentioned above, in polyelectrolyte mesogels the charged B blocks are strongly stretched and form strings of blobs of equal size $\xi_s \approx am^{1/2}$. A similar blob picture refers to a neutral Gaussian chain stretched by an external force, $f = kT/\xi_s$. (The role of this external force in our case is played by the osmotic pressure of mobile counterions.) The behavior of a neutral brush upon stretching was considered in ref 20. It was shown that the transition between collapsed and stretched states of a brush takes place when the value of the force

$$f_t \cong kT|v|/a \qquad (21)$$

provides the equality of sizes of a stretching blob, ξ_s, and that in the collapsed state, $\xi_c \approx a|v|^{-1}$,

$$\xi_s \cong \xi_c \qquad (22)$$

Thus, one obtains for the transition point in a charged mesogel within the accuracy of a numerical prefactor,

$$|v_0| \cong a/\xi_s \cong 1/\sqrt{m} \qquad (23)$$

for all morphologies i. For $i = 1$ (planar layer) this result was obtained earlier in ref 10. A similar scaling dependence of the transition point $|v_0|$ on the charge density $1/m$ was obtained also for conventional polyelectrolyte networks[21] and networks formed by linked polyelectrolyte stars.[22]

Figure 3 shows schematically the dependence of the equilibrium swelling concentration, ϕ^*, of a charged mesogel on the solvent strength. The jumpwise increase

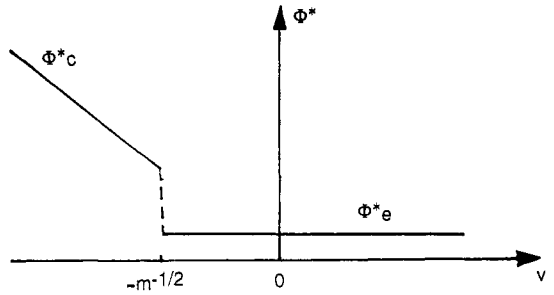

Figure 3. Schematic representation of ϕ^* against the solvent strength (second virial coefficient v) in charged mesogels.

in ϕ^* up to $\phi_c^* \cong |v|$ occurs at the transition point $|v_0| \cong 1/\sqrt{m}$. The value of this jump depends on the morphology of the mesogel and can be estimated using eq 13 for ϕ_e^*. The plot in Figure 3 was drawn based on asymptotical power laws for ϕ_e^* and ϕ_c^*, i.e., ignoring nonpower dependencies which will smooth partly the curve but the abrupt transition will still take place.

Salt Effect. Addition of low molecular weight salt in solution screens electrostatic interactions and diminishes the manifestation of polyelectrolyte effects in polymer brushes.[9,10,22-25] It was shown that, when the concentration of salt ions exceeds by far the concentration of their own counterions in the brush, the so-called salt-dominant regime takes place. In this regime the electrostatic interactions can be described by an effective virial coefficient of interactions between polymer units,

$$v_{el} \cong 1/m^2\phi_s \tag{24}$$

where $\phi_s a^{-3}$ is the concentration of salt in the bulk of the solution. Thus, the brush thickness scales in the salt-dominant regime as $H \cong aNv_{el}^{1/3}(\sigma/a^2)^{-1/3} \propto \phi_s^{-1/3}$. A more refined picture of polyelectrolyte solutions developed by Khokhlov[26] suggests the existence of additional regimes of brush behavior with different dependencies of H on m and ϕ_s. Ross and Pincus[19] also expect $H \sim \phi_s^{-1/2}$ in a certain range of ϕ_s. A recent scaling analysis[27] utilizing the revised picture of screening effects in polyelectrolyte solutions due to Barrat and Joanny[28] showed, however, that the dependence $H \propto v_{el}^{1/3}$ is valid in a wide range of salt contents provided that the elasticity of the grafted chains is Gaussian. Thus, under the conditions of a Θ or marginal good solvent salt effects in a polyelectrolyte brush can be accounted for through the effective virial coefficient given by eq 24. In good solvents, where chains are locally swollen and their response obeys Pincus law,[29] the situation is more complicated.[27] In this paper we do not consider the scaling regime of good solvents and use eq 24 to incorporate salt effects. Thus, polyelectrolyte mesogels in a salt-dominant regime can be considered as neutral mesogels with renormalized second virial coefficient $v' = v + v_{el}$, and their characteristics can be obtained from those for neutral mesogels (Table I).

Deformation of Charged Mesogels. Let us now consider the behavior of charged salt-free mesogels under static deformation. Evidently, it must depend on whether a free, nondeformed mesogel is in a swollen or collapsed state. As before we focus mainly on the case of a "single crystal" lamellar mesogel with aligned lamellar layers and consider here normal deformations (i.e., stretching and compression of a mesogel normally to the interfaces) and shear of swollen lamellar layers with respect to each other.

As was discussed above, in poor solvents charged mesogels are stabilized against attractive pair interactions by electrostatic repulsion and collapse only when $|v| > |v_0| \cong 1/\sqrt{m}$. At $|v| < |v_0|$ gels are swollen due to the osmotic pressure of their counterions and their stretching or compression should provide smooth stress–strain dependencies. The situation is different for collapsed gels, $|v| > |v_0|$, where polyelectrolyte effects are suppressed by strong attractive interactions between units and the system is quasineutral. Here one can expect a jumpwise increase in dimensions via stretching as in a neutral mesogel.[5] The transition point can be determined by equating chemical potentials in stretched and collapsed states. Following the lines of ref 5, the chemical potential μ_s in a stretched state is given at $|v| \gg |v_0|$ by

$$\mu_s \cong -\left(\frac{a}{\xi_s}\right)^2 + \frac{1}{m}\ln\left(\frac{a\xi_s}{\sigma m}\right) \tag{25}$$

where the first term accounts for elastic stretching ($\xi_s \approx Na^2/H_s$) whereas the second term incorporates the translational entropy of counterions (contribution of nonelectrostatic interactions is neglected here). In a collapsed state, where stretching is negligible,

$$\mu_c \cong -\left(\frac{a}{\xi_c}\right)^2 + \frac{1}{m}\ln\left(\frac{a}{\xi_c m}\right) \tag{26}$$

where the first term accounts for nonelectrostatic (attractive) volume interactions and the second term is again due to counterions. Equating $\mu_s = \mu_c$, one obtains

$$\xi_s \cong \xi_c\left[1 - \frac{\xi_c^2}{a^2 m}\ln\left(\frac{\sigma}{\xi_c\xi_s}\right)\right]^{-1/2} \cong \frac{a}{|v|}\frac{1}{\left[1 - \left(\frac{v}{v_0}\right)^2\ln\left(\frac{\sigma}{\xi_s\xi_c}\right)\right]^{1/2}} \tag{27}$$

Since $\ln(\sigma/\xi_c\xi_s) > 0$ in the considered range of parameters $|v| \gg |v_0|$, $\xi_s \geq \xi_c$.

Thus, within the primitive scaling consideration the transition point is specified by condition (22) for both neutral and charged mesogels. The value of the external force, f_t, causing the transition, however, differs from that given by eq 21. It can be obtained by balancing the elastic force, $f_{el} \approx kT/\xi_s$, with the osmotic pressure of the counterions, $f_{ion} \approx kT\xi_s/ma^2$, in a stretched state,

$$\frac{kT}{\xi_s} = \frac{kT\xi_s}{ma^2} + f_t \tag{28}$$

Combined with eq 22, eq 28 gives

$$f_t \cong \frac{kT}{\xi_c}\left(1 - \frac{\xi_c^2}{ma^2}\right) \cong |v|\frac{kT}{a}\left[1 - \left(\frac{v_0}{v}\right)^2\right] \tag{29}$$

Thus, stretching of a charged mesogel in a poor solvent $|v| > |v_0|$ involves the following states:

(1) At very small deformations a linear response of the system is expected.

(2) At $f = f_t$ a jumpwise increase in the gel dimensions takes place and compact collapsed B blocks are transformed into strings of stretching blobs ($\xi_s = \xi_c$). Depending on the value of v, the value of the force f_t can be rather small. As is seen from eq 29, at $v \to v_0$, $f_t \to 0$, indicating that spontaneous swelling of the mesogel takes place at $v = v_0$. At $|v| \gg |v_0|$, the value of the external force causing the transition approaches that for neutral brushes (eq 21).

(3) Further incresae in $f > f_t$ provides a rearrangement of the blob structure, diminishing of the blob size, ξ_s, according to eq 28 with f_t substituted for f.

Figure 4 shows the scaling diagram of a charged brush under deformation. As the similar diagram for a neutral brush (Figure 2 in ref 5) it is presented in reduced variables: $x = v(\sigma/a^2)^{1/2}$, $y = H/H_\Theta$, where $H_\Theta \approx aN(\sigma/a^2)^{-1/2}$

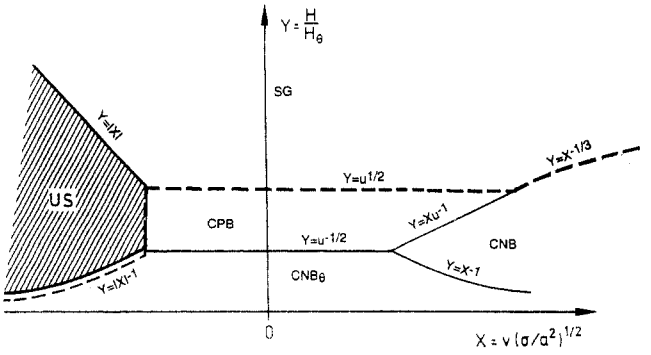

Figure 4. Scaling diagram of a planar polyelectrolyte brush under deformation. (The discussion of the diagram is in the text.)

is the thickness of a neutral brush in a Θ solvent. The parameter $u = \sigma/m \gg 1$ determines the relative degree of brush charging. The dashed line in figure 4 corresponds to the dimensions of a free nondeformed polyelectrolyte brush collapsing at $v = v_0 \approx -m^{-1/2}$ ($x = -u^{1/2}$) from the size $H_e \approx aNm^{-1/2}$ ($y = u^{1/2}$) to the size $H_c \cong aN/\sigma|v|$ ($y = 1/|x|$). Above and below this dashed line the polyelectrolyte brush is stretched or compressed, respectively. The shaded region US corresponds to an unstable regime where the brush thickness changes abruptly from H_c ($y = 1/|x|$) to $H_s \approx Na^2/\xi_s \approx aN|v|$ ($y = |x|$) at a constant value of the external force, f_t, given by eq 29. Above the dashed line brush stretching is governed mainly by the balance of applied force, f, and chain elasticity to give

$$y \cong f\sigma^{1/2}$$

For a compressed brush three regimes are distinguishable within the mean-field approximation used here. At $|v| < |v_0|$ and at relatively small compressions, the response is dominated by the osmotic pressure of counterions (region CPB)

$$y \cong u(f\sigma^{1/2})^{-1}$$

At strong compressions where nonelectrostatic interactions dominate, the balance of the external force and the osmotic pressure due to repulsive pair interactions (region CNB) or ternary interactions (region CNB_θ) provides

$$y \cong x^{1/2}(f\sigma^{1/2})^{-1/2} \text{ (CNB)}$$

$$y \cong (f\sigma^{1/2})^{-1/3} \text{ (CNB}_\theta\text{)}$$

At $u = \sigma/m = 1$ the diagram transforms into that for a neutral brush. (Note that, since scaling regimes of a good solvent are not considered in this paper, corresponding regimes are also absent in the diagram of Figure 4.)

IV. SCF Theory of a Charged Lamellar Mesogel

The scaling-type analysis presented in the previous section provides a rather rough picture of charged mesogels, ignoring fine details of their structure. In this section more refined self-consistent-field theory is developed in order to analyze in detail the structural organization of swelling layers and consider the q dependence of the gel parameters: the equilibrium swelling concentration, ϕ^*, and the elastic and shear moduli. As in ref 5 we focus on the case of lamellar mesogels immersed in a good (or Θ) solvent.

Figure 5 shows schematically the structure of swollen B layers consisting of loops and bridging chains and subjected to normal and tangential deformations. Due to the strong stretching of B blocks each free loop is

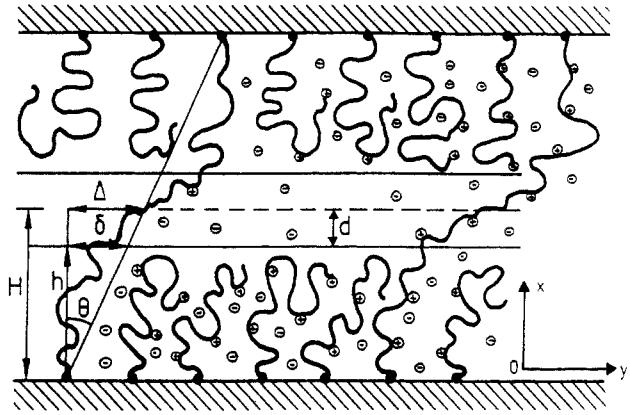

Figure 5. Scheme of a swelling element of a lamellar charged mesogel.

substituted by two grafted chains consisting of $N = N_B/2$ units. Entangled loops are replaced by two bridging chains. The existence of bridging chains leads to the appearance of the so-called central dead zone containing the segments of only bridging chains (loops are excluded from this zone and are located in boundary layers).

As before,[5] it is sufficient to consider half a layer comprised of a boundary layer and a central region. Following the notations of ref 5, the free energy per chain, F, is comprised of contributions associated with these two regions,

$$F = F_b + F_c \tag{30}$$

Segments of bridging chains in the central region are uniformly stretched and the volume fraction of monomers within this region, ϕ_c, is thus constant,

$$\phi_c = \frac{q(N-N')a^3}{\sigma(H-h)} \tag{31}$$

where $N-N'$ is the number of chain units in a central zone of width $d = H-h$ and q is the fraction of bridging chains.

Local electroneutrality of the system is provided by $(N-N')/m$ counterions per chain distributed in the central region. Thus, F_c is given by

$$F_c = \frac{3q(H-h)^2}{2a^2(N-N')} + \frac{3q(\Delta-\delta)^2}{2a^2(N-N')} + \frac{qv(N-N')^2a^3}{\sigma(H-h)} + \frac{N-N'}{m}\ln\left(\frac{\phi_c}{m}\right) \tag{32}$$

The two first terms in eq 32 account for normal and tangential stretching of bridging segments, the third term accounts for binary nonelectrostatic interactions, and the last term is due to the translational entropy of mobile counterions. As was shown above this last contribution dominates over nonelectrostatic volume interactions in a wide range of solvent strengths and we omit nonelectrostatic contributions from further considerations.

The boundary layer contribution

$$F_b = \frac{3(1-q)}{2a^2}\int_0^h g(\eta)\,d\eta\int_0^\eta E_n(x,\eta)\,dx + \frac{3q}{2a^2}\int_0^h E_b(x)\,dx + \frac{3q}{2a^2}\int_0^\delta E_{bT}(y)\,dy + \frac{\sigma}{a^3}\int_0^h \frac{\phi(x)}{m}\ln\left(\frac{\phi(x)}{m}\right)dx \tag{33}$$

where E_n and E_b are normal stretching functions (dx/dn) of nonbridging and bridging chains, respectively, $E_{bT} = dy/dn$ is the tangential stretching function of bridging chains, $g(\eta)$ is the distribution function of the free ends of nonbridging chains, η being the coordinate of the free

end, and $\phi(x)$ is the total profile of polymer units in the boundary layer.

The functional (30)–(33) must be minimized under the following constraints

$$\int_0^{\eta} \frac{1}{E_n(x,\eta)}\,dx = N \tag{34}$$

$$\int_0^{h} \frac{dx}{E_b(x)} = \int_0^{\delta} \frac{dy}{E_{bT}(y)} = N' \tag{35}$$

$$\frac{\sigma}{a^3}\int_0^{h} \phi(x)\,dx = (1-q)N + qN' \tag{36}$$

where

$$\phi(x) = \frac{(1-q)a^3}{\sigma}\int_0^{h} \frac{g(x)}{E_n(x,\eta)}\,d\eta + \frac{qa^3}{\sigma}\frac{1}{E_b(x)} \tag{37}$$

and additional conditions of continuity of the profile $\phi(x)$, and all stretching functions E, at $x = h$.

Omitting the details of this minimization procedure (see Appendix II in ref 5 for details), we present here only final results. The stretching functions are given by the same expressions as in ref 5 (eqs IV.14–IV.16 in ref 5),

$$E_n(x,\eta) = \frac{\pi}{2N}(\eta^2 - x^2)^{1/2} \tag{38}$$

$$E_b(x) = \frac{\pi}{2N}\left[\frac{h^2}{\cos^2\left(\frac{\pi\tau}{2}\right)} - x^2\right]^{1/2} \tag{39}$$

$$E_{bT} = \Delta/N \tag{40}$$

where $\tau = (N - N')/N$.

The profile of polymer units, $\phi(x)$, is not parabolic now but is of Gaussian shape in the boundary region

$$\phi(x) = ce^{-(x^2/h_0^2)} \qquad 0 < x < h$$

$$\phi(x) = ce^{-h^2/h_0^2} \qquad h < x < H \tag{41}$$

where $h_0 = a(8/3\pi^2 m)^{1/2}N$, $z = h/h_0$, and c is a normalization constant,

$$c = \frac{(1-q\tau)Na^3}{\sigma h_0}\left(\int_0^{z} e^{-t^2}\,dt\right)^{-1} \tag{42}$$

The distribution function of the free ends can be obtained by inverting eq 37 to give

$$g(\eta) = \frac{(1-q\tau)}{h_0^2(1-q)}\left\{\frac{D[(z^2 - \eta^2/h_0^2)^{1/2}]}{D[z]} + \frac{\left[z^2 - \frac{\eta^2}{h_0^2}\right]^{1/2}}{2\left[\frac{z^2}{\cos^2(\pi\tau/2)} - \frac{\eta^2}{h_0^2}\right]}\right\} \tag{43}$$

where

$$D[t] = e^{-t^2}\int_0^{t} e^{x^2}\,dx$$

is Dawson integral. Finally, the interdependence of q, τ, and z is given by

$$qD[z] = \frac{\pi z}{2}(1-q\tau)\tan\left(\frac{\pi\tau}{2}\right) \tag{44}$$

and

$$H/h_0 = (h+d)/h_0 = z\left[1 + \frac{\pi\tau}{2}\tan\left(\frac{\pi\tau}{2}\right)\right] \tag{45}$$

Relationships (38)–(45) determine the equilibrium characteristics of swollen B layers at given values of H and Δ. Additionally, the condition of mechanical equilibrium requires the balance of the normal and tangential pressures at $x = 0$ (the surface of the insoluble A domain).

Force Balance. Balancing the normal elastic force $f_{el}(x=0)$ with the osmotic pressure of counterions and the normal component of applied external force, f_N, one has

$$f_{el}(x=0) + f_N = f_{ion}(x=0) \tag{46}$$

and the tangential pressure balance is

$$f_T = 3qkTa^{-2}(\Delta/N) \tag{47}$$

Taking into account eq 41, the osmotic force due to mobile counterions is given by

$$f_{ion}(x=0) = \phi(x=0)\frac{\sigma}{ma^3} = \frac{ckT\sigma}{ma^3} \tag{48}$$

The elastic force acting at the surface of the insoluble A domain can be calculated following the lines of ref 5 (using eqs V.3 and V.4 in ref 5),

$$f_{el}(x=0) = \frac{3(1-q)}{a^2}\int_0^{h} g(\eta)\,E(0,\eta)\,d\eta + \frac{3q}{a^2}E_b(0) = kT\left[\frac{c\sigma}{ma^3}(1 - e^{-z^2}) + \frac{3qa}{c\sigma}e^{z^2}\right] \tag{49}$$

Thus, the mechanical equilibrium of normal forces gives

$$f_N/kT = \frac{c\sigma}{ma^3}e^{-z^2} - \frac{3aq^2}{c\sigma}e^{z^2} \tag{50}$$

where $f_N > 0$ and $f_N < 0$ refers to compression and stretching, respectively. Introducing reduced normal and tangential components of stresses,

$$U_{N,T} = 4\pi f_{N,T}\frac{Na^2}{h_0 kT}$$

and using eqs 42 and 44, one can rewrite eqs 50 and 47 as

$$U_N/q = -2z\tan\left(\frac{\pi\tau}{2}\right) + \frac{1}{z\tan\left(\frac{\pi\tau}{2}\right)} \tag{51}$$

$$U_T/q = 12\pi t \tag{52}$$

where $t = \Delta/h_0$.

Thus, eqs 51, 52, and 44 determine the equilibrium parameters of swelling B layers, z, τ, and H/h_0, at given values of q, f_N, and f_T.

Nondeformed Mesogel. For normally undeformed mesogel ($U_N = 0$), eq 51 gives

$$z\tan\left(\frac{\pi\tau}{2}\right) = \frac{1}{\sqrt{2}} \tag{53}$$

Together with eq 44 it gives the equilibrium dependences $z^*(q)$ and $\tau^*(q)$ plotted in Figures 6 and 7 by dashed lines. The corresponding behavior of the total thickness, given by eq 45, is presented in Figure 8. As is seen from Figures 6–8, qualitatively the behavior of a charged mesogel resembles that of a neutral one: with q increasing z^* and H^* decrease, while τ^* increases. At small q values, however, z^* and H^* tend to infinity, whereas for neutral mesogels z^* and H^*/H_0 tend to unity. The divergence of z^* (and H^*) at $q = 0$ is due to the fact that the analytical SCF theory presented in this section does not take into account the finite extensibility of the polyelectrolyte blocks. As was already mentioned in ref 22, within the Gaussian approximation for the stretching entropy, the upper boundary of a free ($q = 0$) polyelectrolute brush is $H = \infty$. However, this descrepancy does effect neither the scaling

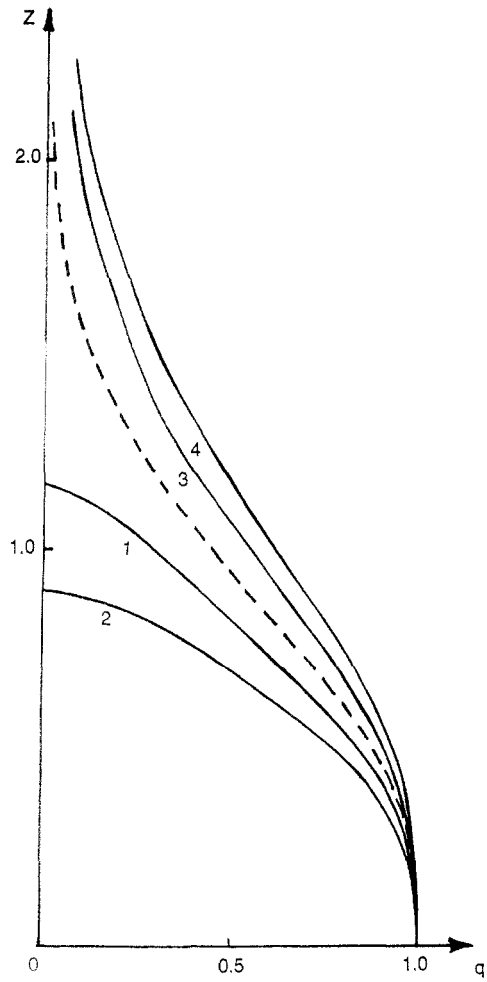

Figure 6. Dependence of the relative thickness of the boundary layer z on the fraction of bridging chains, q, at various deformations: $U_N = 0.5$ (1), 1.0 (2), −0.5 (3), and −1.0 (4). The dashed line corresponds to a nondeformed system, $U_N = 0$.

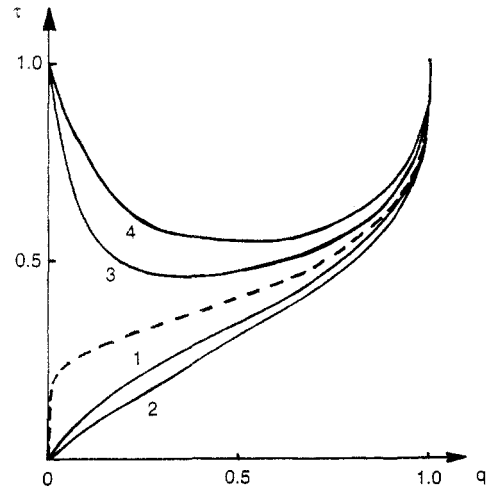

Figure 7. Dependence of the relative number of units in the dead zone τ on the fraction q of bridging chains at various deformations. The values of U_N are the same as in Figure 6; the dashed line corresponds to $U_N = 0$.

behavior nor the polymer units distribution in the brush to a large extent, since the distribution function of the free ends quickly decays to the periphery of the brush and the error due to chains stretched above their counterlength Na is negligible.

In our case the existence of bridging chains provides $H < Na$ in a wide range of q values, $q > q_{cr}$. (At $q < q_{cr}$ the theory predicts unrealistic stretching of bridging chains

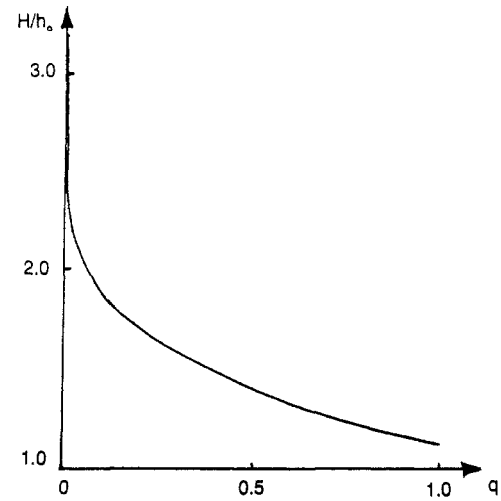

Figure 8. Dependence of the nondeformed layer thickness, H/h_0, on the fraction q of bridging chains.

$H > Na$.) In order to estimate q_{cr}, we consider the stretching function $E_b(x)$ of bridging chains. It follows from eq 39 that the bridging chains are stretched nonuniformly: stretching is maximal in the boundary layers near the surface of the A domain ($x = 0$) and decreases to the center of the swelling layers. In the central region the segments of bridging chains are stretched uniformly and their degree of stretching is

$$\frac{d}{aN\tau} = \frac{\pi z}{2N}\tan\left(\frac{\pi\tau}{2}\right) = \frac{1}{(3m)^{1/2}}$$

under equilibrium conditions. Hence, in order to provide $E_b(0) \ll 1$ and thus to justify the Gaussian expression for the stretching entropy, the condition

$$E_b(0) = \frac{\pi z h_0}{2N\cos(\pi\tau/2)} = \left[\frac{2z^2+1}{3m}\right]^{1/2} \ll 1 \qquad (54)$$

must be fulfilled. It follows from eq 44 that, at small q values, $q \to 0$, z scales as

$$z \approx \left[\ln\left(\frac{(\pi/8)^{1/2}}{q}\right)\right]^{1/2} \qquad (55)$$

Thus, taking into account eqs 54 and 55, q_{cr} can be estimated as

$$q_{cr} \approx \left(\frac{\pi}{8}\right)^{1/2} e^{(1-3m)/2} \qquad (56)$$

For weakly charged chains $m \gg 1$ q_{cr} is exponentially small, and thus the SCF approach can in practice be used in the wide range of q values. (Addition of low molecular weight salt diminishes the electrostatic stretching of the charged blocks, $H < \infty$, and takes away any restrictions on the q values.)

Elastic and Shear Moduli. At small deformations the Hookean behavior of lamellar mesogels is characterized by Young's and shear moduli. For normal stress $P_N = f_N/\sigma$ and normal strain of $\epsilon = (H - H^*)/H^* \ll 1$ Young's modulus

$$E = dP_N/d\epsilon$$

can be calculated using eqs 51, 44, and 45. In the limit of small q values, $q_{cr} \ll q \ll 1$,

$$\frac{Ea^3}{kT} \approx \frac{ah_0qz^*}{\pi\sigma N} \approx \frac{q\phi_0}{m}\left[\ln\left(\frac{\pi}{8q^2}\right)\right]^{1/2} \qquad (57)$$

where $\phi_0 = Na^3/\sigma h_0$ is proportional to the average concentration of polymer units in a free undeformed

polyelectrolyte brush with average thickness h_0. Thus, as in a neutral mesogel, Young's modulus of a charged mesogel scales more strongly than just linearly with q,

$$Ea^3/kT \propto q(\ln(1/q))^{1/2}$$

This reflects the complex structure of swelling layers. However, the logarithmic correlation to the linear q dependence of Young's modulus is rather weak, indicating a much stronger stretching of bridging chains in charged mesogels with respect to neutral systems.

The shear modulus of a charged mesogel

$$n = dP_T/dt$$

is easily obtained from eq 52 and is given by

$$\frac{na^3}{kT} = \frac{3qah_0}{\sigma N} \cong \frac{q}{m}\phi_0 \tag{58}$$

Figures 6 and 7 show the dependencies $z(q)$ and $\tau(q)$ at various deformations. Certainly, the picture resembles the behavior of a neutral mesogel.[5] Stretching leads to a considerable increase of the central region particularly at small q values and to a nonmonotonic behavior of $\tau(q)$. Compression results in a monotonic decrease in both z and τ values. At strong compressions, when the nonelectrostatic repulsion between units dominates, the dependencies $z(q)$ and $\tau(q)$ are expected to approach those for neutral mesogels.[5]

The dependencies of z, τ, and H/h_0 on the deformation are shown in Figure 9. It should be noted, however, that as before[5] the effect of entanglements is totally ignored here and, thus, eqs 57 and 58 can be regarded as lower limits of real E and n values.

Salt Effect. The above results refer to a charged mesogel swollen in a salt-free solvent. As was already noted in section III, the effect of salt on the structure of a free polyelectrolyte brush was discussed in refs 9 and 10. It was shown that in a salt-dominant regime of a brush all structural characteristics of a brush coincide with those of a neutral brush with a renormalized virial coefficient of unit interaction, (eq 24). The same conclusion is valid for a swelling element of a charged mesogel. Hence, when the concentration of salt ions, ϕ_s, exceeds by far the concentration of their own counterions in a mesogel, ϕ_0/m, the results of ref 5 with a renormalized second virial coefficient $v' = v + 1/(4m^2\phi_s)$ are applicable. In particular, the profile of polymer units, $\phi(x)$, becomes of parabolic shape in the boundary layers and the equilibrium swelling concentration is given by

$$\phi^* \cong (v')^{-1/3}\left(\frac{\sigma}{a^2}\right)^{-2/3} \cong \left(v + \frac{1}{4m^2\phi_s}\right)^{-1/3}\left(\frac{\sigma}{a^2}\right)^{-2/3} \tag{59}$$

while the elastic and shear moduli now scale as

$$\frac{Ea^3}{kT} \cong v'q^{2/3}(\phi^*)^2 \cong q^{2/3}\left(\frac{1}{m^2\phi_s}\right)^{1/3}\left(\frac{a^2}{\sigma}\right)^{4/3} \tag{60}$$

$$\frac{na^3}{kT} \cong v'q(\phi^*)^2 \cong q\left(\frac{1}{m^2\phi_s}\right)^{1/3}\left(\frac{a^2}{\sigma}\right)^{4/3} \tag{61}$$

At high salt contents, $v \gg 1/(4m^2\phi_s)$, charged mesogels pass into a quasineutral regime, where all electrostatic effects are screened and nonelectrostatic volume interactions determine the equilibrium structure and properties of a mesogel.

V. Discussion

The main purpose of this paper is to present a general theoretical picture of the equilibrium behavior of ionizable block copolymer mesogels. Such systems are interesting by themselves as they are an example of supermolecular networks with a modulated distribution of cross-links (domains of the minor component play the role of individual cross-links, while the bridging chains ensure the connectivity of the whole system). Even more important is that they provide wide opportunities for experimental tests of numerous theoretical predictions concerning the behavior of polymers in restricted geometries (polymer brushes).

The rather difficult experimental problem of creating a neutral polymer brush (by adsorption of anchoring block copolymers,[30] grafting of end-functionalized chains,[31] etc.) becomes even more complicated for charged polymers. Due to long-range electrostatic repulsions between polyelectrolyte chains, charged brushes are expected to be much sparse than neutral ones. Theoretical calculations[32] show, for example, that the surface coverage of adsorbed block copolymers with ionizable nonadsorbing blocks is expected to be an order of magnitude lower than that for neutral block copolymers under similar conditions. Screening electrostatic repulsion between chains by addition of salt leads to a certain increase in the adsorbed amount,[33] but still brushes obtained in this way are rather loose.

The swelling layers of block copolymer mesogels are examples of self-assembling polymer brushes formed due to the incompatibility of long blocks in the process of microphase segregation. Being neutral in the dry melt, they can be charged in the process of mesogel swelling, thus being the experimental realization of polyelectrolyte brushes with a controlled degree of charging.

Measurements of the equilibrium swelling concentrations under various pH conditions and salt contents combined with small-angle scattering techniques can provide unique information on the polyelectrolyte brush behavior in solutions. As was already mentioned above, the theoretical picture of salted polyelectrolyte solutions (and salted polymer brushes) is far from being completely settled. Thus, experimental observations on polyelectrolyte mesogels could provide more insight into the problem. In particular, experimental data on the equilibrium swelling concentrations, ϕ^*, via the salt content, ϕ_s, could probably check the validity of the simplified picture of the salt-dominant regime. Within this picture one expects at $\phi_s \gg \phi_e^*/m$ for the equilibrium swelling concentration (see Table I)

$$\phi^* \sim (v')^{-i/(i+2)} \sim \phi_s^{\,i/(i+2)}$$

Thus, with increasing i the dependence of ϕ^* on ϕ_s becomes more strong and is most pronounced for spherical mesogels ($i = 3$). However, the experimental design of lamellar mesogels is probably more realistic. Here one expects $\phi^* \sim \phi_s^{1/3}$, which is also a rather strong dependence.

As follows from eqs 60 and 61, an increase in the salt content, ϕ_s, leads to diminishing of both elastic moduli in the salt-dominant regime as $E \sim n \sim \phi_s^{-1/3}$. Thus, deviations from this dependence could give some insight into the role of entanglements in swollen mesogels.

A promising set of experiments can be suggested due to variation of solvent strength. As follows from the results of this paper and refs 19 and 22, the collapse of mesogels of various morphologies occurs as phase transition of the first order with a jumpwise decrease of its dimensions below the Θ point. Contrary to neutral mesogels, charged mesogels are expected to be stabilized against collapse in a rather wide range of solvent strengths, $v < 0$. The transition point, $v_0 \approx -m^{-1/2}$, scales similarly for all

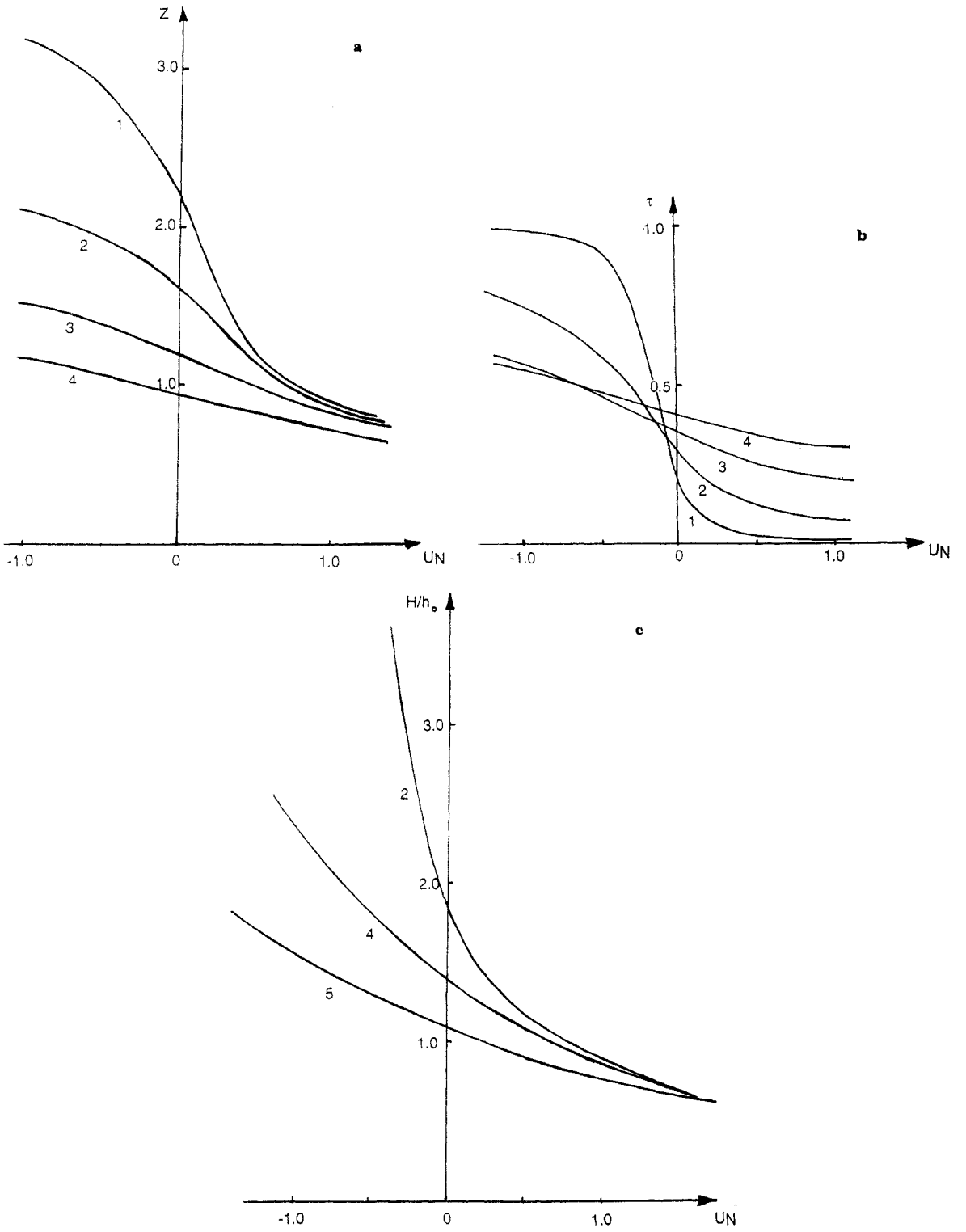

Figure 9. Dependence of z (a), τ (b), and H/h_0 (c) on the value of the reduced normal force U_N at various q values: q = 0.01 (1), 0.1 (2), 0.3 (3), 0.5 (4), and 1.0 (5).

morphologies i and can be shifted by the variation of the degree of charging of the ionizable blocks, $1/m$. The collapse is expected to be most pronounced in a spherical geometry. Indeed, it follows from eqs 13 and 16 (and also results of ref 19) that the value of jump, $\phi_c^*/\phi_e^* \cong (\sigma/a^2)^i k^{i-1} m^{-(1+i)/2}$, increases with i and k). Thus, the strongest manifestation of the collapse is expected for asymmetrical block copolymers in a spherical geometry. In the limit $k \to \infty$ ($N_B \to \infty$) the critical point $m_{cr} \to \infty$, $\phi_{cr} \sim |v_{cr}| \to 0$ for $i = 2$ and 3 (eq 19), while the lower branch of the spinodal, $\phi_2(m) \to 0$, (eq 20). Thus, the gap between both branches of the spinodal increases for cylindrical and spherical mesogels, and in the limit $k \to \infty$ their collapses occur as strong first-order phase transitions.

As was shown for neutral brushes,[11,17] the transition from a swollen to a collapsed state sharpens with the change of geometry from a planar to a spherical brush. Being a cooperative non-phase transition for a planar layer, the collapse of a spherical brush occurs as a phase transition of the second order (as an individual flexible polymer chain). The introduction of an additional swelling factor into the system (osmotic pressure of mobile counterions) contributes mainly to the free energy of a swollen state and makes this transition only more sharp. Thus, as in neutral brushes, the collapse of charged brushes and

mesogels is expected to sharpen with increasing i and occurs as a strong phase transition of the first order for all morphologies.

The scaling picture of charged mesogels presented in this paper is rather rough and ignores nonpower dependencies which can introduce considerable corrections to asymptotical power laws. The SCF theory of section IV provides a more detailed picture of electrostatically swollen mesogels. (SCF analysis of charged brushes was carried out in refs 23–25.)

As in neutral mesogels there are considerable gradients of polymer concentrations throughout swelling layers. Due to the strong stretching of charged blocks central dead zones are well pronounced and occupy a noticeable part of space. In neutral mesogels the central dead zone can be smeared out by fluctuations at small q values, but in charged mesogels the dead zone is well pronounced even below $q = q_{cr} \to 0$. Following the lines of ref 5, the effect of fluctuations can be estimated through the value of the ratio of the penetration length of nonbridging chains into the dead zone, $\xi \cong H(a\sqrt{N}/h)^{4/3}$, and the thickness of the central dead zone, $d = H - h$. At small $q \ll 1$ where $H \approx h$, eqs 44, 53, and 55 give $d/H \cong \tau/z \cong z^{-2} \cong 1/\ln(q^{-1})$, while $\xi/H \cong (a\sqrt{N}/zh_0)^{4/3}$. Correspondingly, the ratio $d/\xi \cong (Q/z)^{2/3} \cong (-Q^2/\ln(q))^{1/3} \gg 1$ at $q \gg e^{-Q^2}$ and, thus, the dead zone is well-defined in the whole range $q > q_{cr}$.

Acknowledgment. The financial support provided by the Netherlands Foundation for Chemical Research (SON) with aid from The Netherlands Organisation for Scientific Research (NWO) and the hospitality of Prof. G. Fleer at Wageningen Agricultural University are acknowledged with gratitude. Critical reading of the manuscript by Dr. O. Borisov and Dr. F. A. M. Leermakers is highly appreciated.

References and Notes

(1) Gallot, B. In *Liquid Crystalline Order in Polymers*; Blumstein, A., Ed.; Academic Press: New York, 1978.
(2) Keller, A.; Odell, J. A. In *Processing, Structure and Properties of Block Copolymers*; Folkes, M. J., Ed.; Elsevier: New York, 1985.
(3) Douy, A.; Gallot, B. *Makromol. Chem.* **1972**, *156*, 81.
(4) Halperin, A.; Zhulina, E. B. *Europhys. Lett.* **1991**, *16*, 337.
(5) Zhulina, E. B.; Halperin, A. *Macromolecules* **1992**, *25*, 5730.
(6) Semenov, A. N. *Sov. Phys. JETP* **1985**, *61*, 731.
(7) Skvortsov, A. M.; Pavlushkov, I. V.; Gorbunov, A. A.; Zhulina, E. B.; Borisov, O. V.; Priamitsyn, V. A. *Polym. Sci. USSR* **1988**, *30*, 1706. Zhulina, E. B.; Priamitsyn, V. A.; Borisov, O. V. *Polym. Sci. USSR* **1989**, *31*, 205.
(8) Milner, S. T.; Witten, T. A.; Cates, M. E. *Europhys. Lett.* **1988**, *5*, 413; *Macromolecules* **1988**, *21*, 2610.
(9) Pincus, P. *Macromolecules* **1991**, *24*, 2912.
(10) Borisov, O. V.; Birshtein, T. M.; Zhulina, E. B. *J. Phys. II* **1991**, *1*, 521.
(11) Zhulina, E. B.; Borisov, O. V.; Priamitsyn, V. A.; Birshtein, T. M. *Macromolecules* **1991**, *24*, 140.
(12) Odijk, T. *J. Polym. Sci., Polym. Phys. Ed.* **1977**, *15*, 447. Skolnick, J.; Fixman, M. *Macromolecules* **1977**, *10*, 944.
(13) Nyrkova, I. A.; Khokhlov, A. R.; Kramarenko, E. Yu. *Polym. Sci. USSR* **1990**, *32*, 852. Nyrkova, I. A.; Khokhlov, A. R. *Macromolecules* **1992**, *25*, 1493.
(14) Marko, J. F.; Rabin, Y. *Macromolecules* **1992**, *25*, 1503.
(15) Daoud, M.; Cotton, J. P. *J. Phys. (Paris)* **1982**, *43*, 531.
(16) Birshtein, T. M.; Zhulina, E. B. *Polymer* **1984**, *25*, 1453.
(17) Borisov, O. V.; Birshtein, T. M.; Zhulina, E. B. *Polym. Sci. USSR* **1988**, *30*, 767.
(18) Halperin, A. *J. Phys. (Paris)* **1988**, *47*, 547.
(19) Ross, R. S.; Pincus, P. *Macromolecules* **1992**, *25*, 1503.
(20) Halperin, A.; Zhulina, E. B. *Macromolecules* **1991**, *24*, 5393.
(21) Tanaka, T.; Fillmore, D.; Sun, S. T.; Nishio, I.; Swislow, G.; Shan, A. *Phys. Rev. Lett.* **1980**, *45*, 1636. Vasilevskaya, V. A.; Khokhlov, A. R. In *Mathematical Methods in Polymers*; USSR Academy of Science Biological Research Center: 1982; p 45.
(22) Borisov, O. V.; Birshtein, T. M.; Zhulina, E. B. *Prog. Colloid Polym. Sci.* **1992**, *90*, 177.
(23) Zhulina, E. B.; Borisov, O. V.; Birshtein, T. M. *J. Phys. II (Paris)* **1992**, *2*, 63.
(24) Miklavic, S. J.; Marcelja, S. *J. Phys. Chem.* **1988**, *92*, 6718.
(25) Misra, S.; Varanasi, S.; Varanasi, P. P. *Macromolecules* **1989**, *22*, 4173.
(26) Grosberg, A. Yu.; Khokhlov, A. R. *Statistical Physics of Macromolecules*; Nauka: Moscow, 1989.
(27) Borisov, O. V.; Zhulina, E. B.; Birshtein, T. M. Submitted for publication in *J. Phys. II (Paris)*.
(28) Barrat, J. L.; Joanny, J. F. Preprint.
(29) Pincus, P. *Macromolecules* **1976**, *9*, 386.
(30) Hadziioannou, G.; Patel, S.; Granick, S.; Tirrell, M. *J. Am. Chem. Soc.* **1986**, *108*, 2869. Tirrell, M.; Patel, S.; Hadziioannou, G. *Proc. Natl. Acad. Sci. U.S.A.* **1987**, *84*, 472.
(31) Auroy, P.; Auvray, L.; Leger, L. *Phys. Rev. Lett.* **1991**, *66*, 719; *Macromolecules* **1991**, *24*, 2523.
(32) Israels, R.; Scheutjens, J.; Fleer, G. Submitted for publication in *Macromolecules*.
(33) Argillier, J. F.; Tirrell, M. Preprint.